Electronic Supporting Information

Mercury Ion-DNA Specificity Triggers a Distinctive Photoluminescence Depression in Organic Semiconductor Probes Guided with Thymine-Rich Oligonucleotide Sequence.

Jietao Huang[a,1], Jin Hyuk Park [b,1], Seung Hyuk Back[c], Yuhui Feng[d], Chunzhi Cui[a,*], Long Yi Jin[a,*], and Dong June Ahn[b,c,*]

In this Supplementary Information, the following results are presented:

Fig. S1. A scanning electron microscopy (SEM) image of the Alq_3 particles prepared in pure deionized (D.I.) water not containing single-strand DNA (ssDNA).

Fig. S2. Quantitative green pixel values of visible PL images of ssDNA-guided Alq_3 rods after interaction with mercury ions [Fig. 2(a)].

Fig. S3. Quantitative PL graph of log-intensity versus time and fitting kinetic data using Equation (2).

Fig. S4. The distinctive depression of luminescence of three different Alq_3 particles with thymine-rich ssDNA before and after interaction with mercury ions

Fig. S5. Luminescence response of Alq_3 particles with three different sequences of ssDNA: (a) PL spectra and (b) quantitative PL intensities.

Fig. S6. PL spectra of the ssDNA-guided Alq_3 microrods incubated in D.I. water at 50°C for 30 min and then returned to room temperature.

Mov. S1. Phenomena of a real-time reduction in the luminescence of ssDNA-guided Alq_3 rods for 60 min before exposure to mercury solutions

Mov. S2. Phenomena of a real-time reduction in the luminescence of ssDNA-guided Alq_3 rods for 60 min after exposure to mercury solutions.

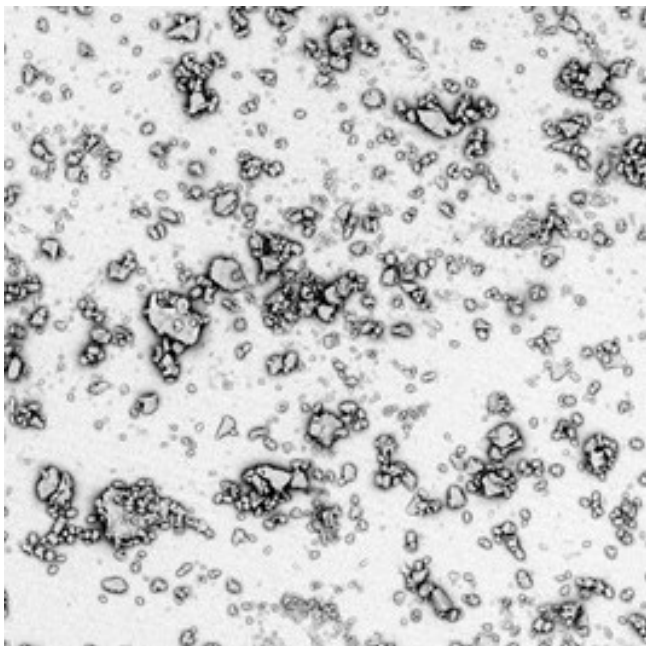

Fig. S1. A scanning electron microscopy (SEM) image of the Alq_3 particles prepared in pure deionized (D.I.) water not containing single-strand DNA (ssDNA). An irregular macroscopic shape of the Alq3 particles was observed**.**

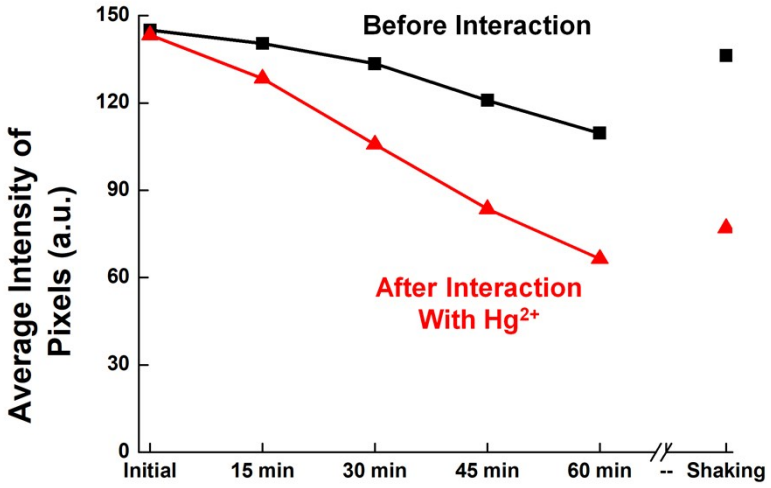

Fig. S2. Quantitative green pixel values of visible PL images of ssDNA-guided Alq_3 rods after interaction with mercury ions [Figure 2(a)]. This pixel values were measured with Adobe Photoshop CS5 program. Average intensity of ssDNA-guided Alq_3 rods slightly decreased before exposure to mercury (Ⅱ) chloride solution. Of note, the intensity of samples after exposure to a mercury (Ⅱ) chloride solution continuously drastically decreased.

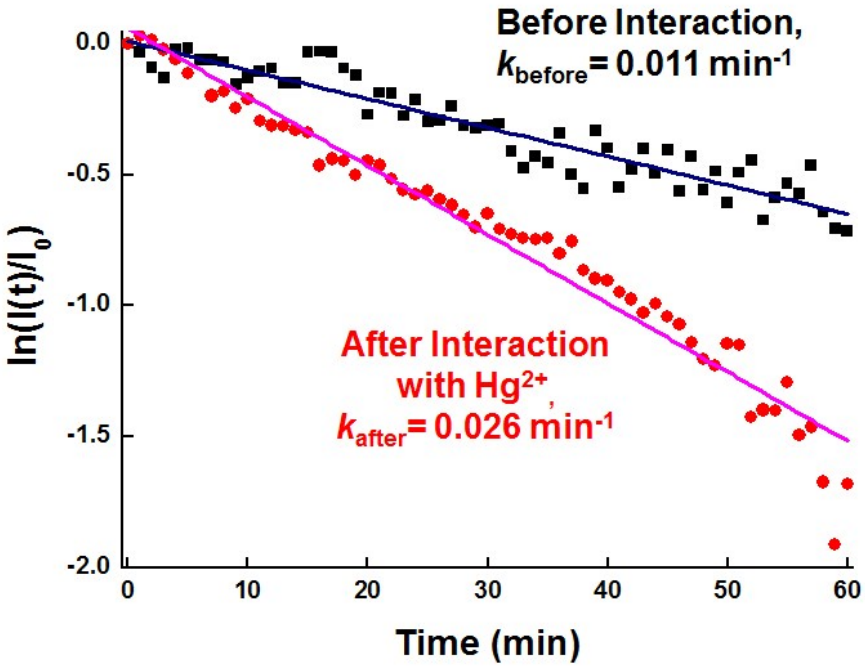

Fig. S3. Quantitative PL graph of log-intensity versus time and fitting kinetic data using Equation (2). PL kinetics and fitting graph of ssDNA-guided Alq_3 rods before (black curve) and after interaction with mercury ions (red curve). PL spectra were analyzed with excitation by a 365 nm laser and emission at a 512 nm wavelength. Equation (2) is as follows:

$$\ln\left(\frac{I(t)}{I_0}\right) = -kt \tag{2}$$

which are governed by the kinetic decay constant k and initial fluorescence intensity I_0.

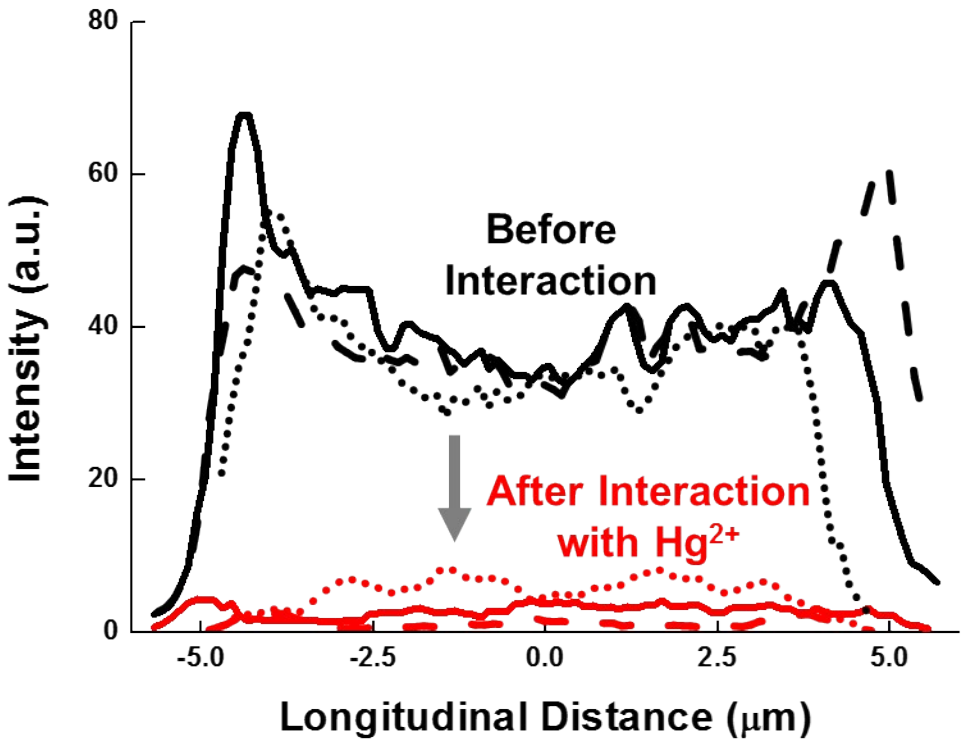

Fig. S4. The distinctive depression of luminescence of three different Alq_3 particles with thymine-rich ssDNA before and after interaction with mercury ions

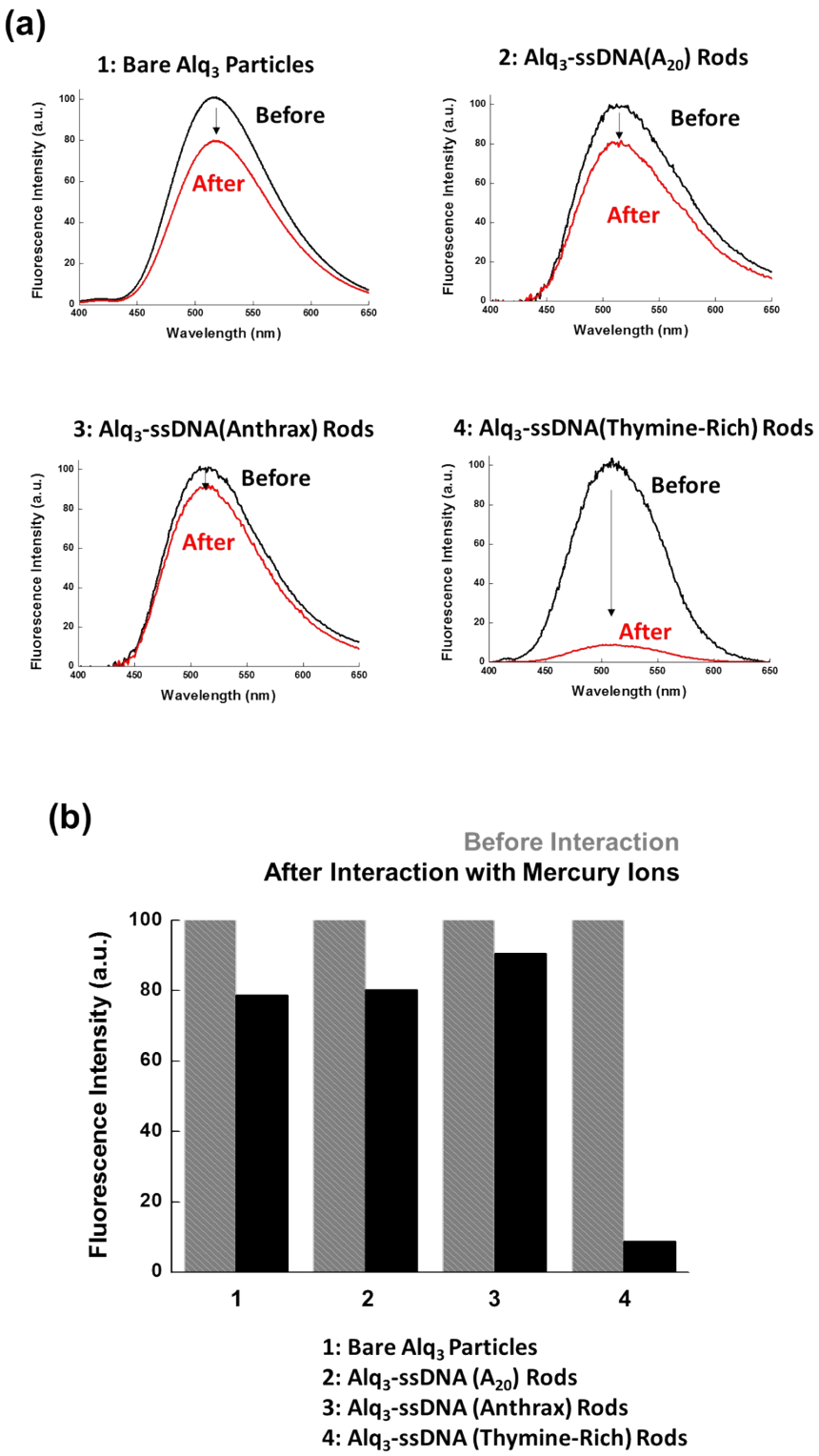

Fig. S5. Luminescence response of Alq_3 particles with three different sequences of ssDNA: (a) PL spectra and (b) quantitative PL intensities. The sequences of ssDNA(A_{20}) and ssDNA(Anthrax) are 5`-AAAAAAAAAAAAAAAAAAAA-3`and 5`-ATCCTTATCATTATTTAACAATAATCC-3`, respectively.

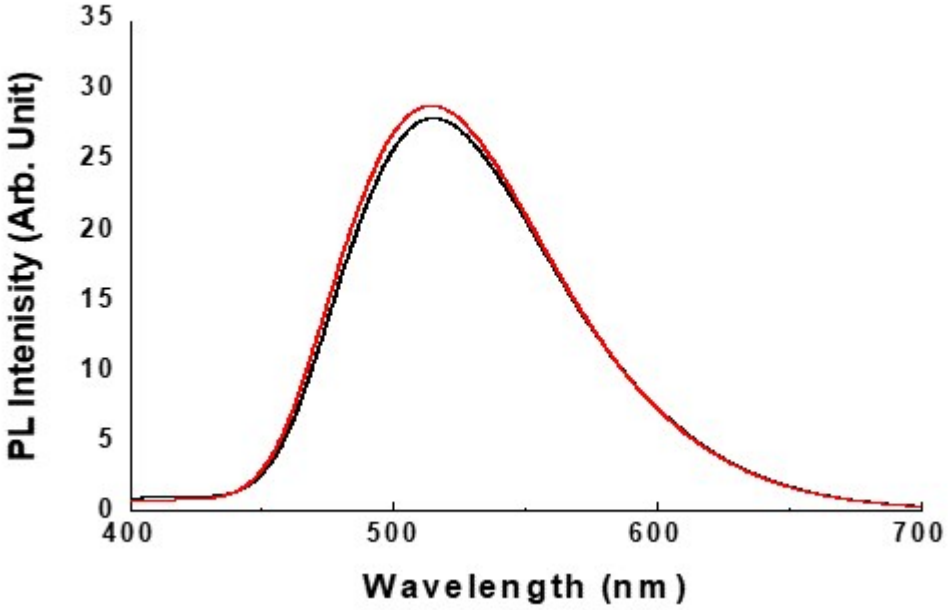

Fig. S6. PL spectra of the ssDNA-guided Alq_3 microrods incubated in D.I. water at 50°C for 30 min and then returned to room temperature. PL spectra of the Alq_3 rods before (black curve) and after thermal treatment at 50 °C for 30 min, followed by a return to room temperature (red curve). PL intensity of the Alq_3 rods persisted after thermal treatment at 50°C for 30 min.